

# Deterministic phase engineering for optical Fano resonances with arbitrary lineshape and frequencies

Jiao Lin,<sup>1,2</sup> Lujun Huang,<sup>1</sup> Yiling Yu,<sup>3</sup> Sailing He,<sup>2</sup> and Linyou Cao<sup>1,3\*</sup>

<sup>1</sup>Department of Materials Science and Engineering, North Carolina State University, Raleigh NC 27695, USA

<sup>2</sup>State Key Laboratory of Modern Optical Instrumentations, Centre for Optical and Electromagnetic Research, Zhejiang University, Zijingang campus, Hangzhou 310058, China

<sup>3</sup>Department of Physics, North Carolina State University, Raleigh NC 27695, USA

\*[lcao2@ncsu.edu](mailto:lcao2@ncsu.edu)

**Abstract:** We present an approach of deterministic phase engineering that can enable the rational design of optical Fano resonances with arbitrarily pre-specified lineshapes. Unlike all the approaches previously used to design optical Fano resonances, which fall short of designing the resonances with arbitrary lineshapes because of the lack of information for the optical phases involved, we develop our approach by capitalizing on unambiguous knowledge for the phase of optical modes. Optical Fano resonances arise from the interference of photons interacting with two optical modes with substantially different quality factors. We find that the phase difference of the two modes involved in optical Fano resonances is determined by the eigenfrequency difference of the modes. This allows us to deterministically engineer the phase by tuning the eigenfrequency, which may be very straightforward. We use dielectric grating structures as an example to illustrate the notion of deterministic engineering for the design of optical Fano resonances with arbitrarily pre-specified symmetry, linewidth, and wavelengths.

© 2015 Optical Society of America

OCIS codes: (290.5825) Scattering theory; (260.5740) Resonance; (160.4236) Nanomaterials.

---

## References and links

1. C. Debus and P. Haring Bolívar, "Terahertz biosensors based on double split ring arrays," *Proc. SPIE* **6987**, 69870U (2008).
2. F. Hao, P. Nordlander, Y. Sonnefraud, P. Van Dorpe, and S. A. Maier, "Tunability of subradiant dipolar and Fano-type plasmon resonances in metallic ring/disk cavities: implications for nanoscale optical sensing," *ACS Nano* **3**(3), 643–652 (2009).
3. N. Liu, T. Weiss, M. Mesch, L. Langguth, U. Eigenthaler, M. Hirscher, C. Sönnichsen, and H. Giessen, "Planar metamaterial analogue of electromagnetically induced transparency for plasmonic sensing," *Nano Lett.* **10**(4), 1103–1107 (2010).
4. N. Verellen, P. Van Dorpe, C. Huang, K. Lodewijks, G. A. E. Vandenbosch, L. Lagae, and V. V. Moshchalkov, "Plasmon line shaping using nanocrosses for high sensitivity localized surface plasmon resonance sensing," *Nano Lett.* **11**(2), 391–397 (2011).
5. S. Zhang, K. Bao, N. J. Halas, H. Xu, and P. Nordlander, "Substrate-induced Fano resonances of a plasmonic nanocube: a route to increased-sensitivity localized surface plasmon resonance sensors revealed," *Nano Lett.* **11**(4), 1657–1663 (2011).
6. V. A. Fedotov, M. Rose, S. L. Prosvirnin, N. Papasimakis, and N. I. Zheludev, "Sharp trapped-mode resonances in planar metamaterials with a broken structural symmetry," *Phys. Rev. Lett.* **99**(14), 147401 (2007).
7. N. I. Zheludev, S. L. Prosvirnin, N. Papasimakis, and V. A. Fedotov, "Lasing spaser," *Nat. Photonics* **2**(6), 351–354 (2008).
8. N. Papasimakis and N. I. Zheludev, "Metamaterial-induced transparency: sharp Fano resonances and slow light," *Opt. Photonics News* **20**(10), 22–27 (2009).
9. S. F. Mingaleev, A. E. Miroshnichenko, Y. S. Kivshar, and K. Busch, "All-optical switching, bistability, and slow-light transmission in photonic crystal waveguide-resonator structures," *Phys. Rev. E Stat. Nonlin. Soft Matter Phys.* **74**(4), 046603 (2006).

10. Z. L. Sámson, K. F. MacDonald, F. De Angelis, B. Gholipour, K. Knight, C. C. Huang, E. Di Fabrizio, D. W. Hewak, and N. I. Zheludev, "Metamaterial electro-optic switch of nanoscale thickness," *Appl. Phys. Lett.* **96**(14), 143105 (2010).
11. W.-S. Chang, J. B. Lassiter, P. Swanglap, H. Sobhani, S. Khatua, P. Nordlander, N. J. Halas, and S. Link, "A plasmonic Fano switch," *Nano Lett.* **12**(9), 4977–4982 (2012).
12. M. Heuck, P. T. Kristensen, Y. Elesin, and J. Mørk, "Improved switching using Fano resonances in photonic crystal structures," *Opt. Lett.* **38**(14), 2466–2468 (2013).
13. A. Ahmadvand, S. Golmohammadi, M. Karabiyik, and N. Pala, "Self-assembled silicon-based clusters to design efficient, fast, and controllable Fano switches," *Microw. Opt. Technol. Lett.* **57**(5), 1242–1246 (2015).
14. M. V. Rybin, D. S. Filonov, P. A. Belov, Y. S. Kivshar, and M. F. Limonov, "Switching from visibility to invisibility via Fano resonances: theory and experiment," *Sci. Rep.* **5**, 8774 (2015).
15. N. Dabidian, I. Kholmanov, A. B. Khanikaev, K. Tatar, S. Trendafilov, S. H. Mousavi, C. Magnuson, R. S. Ruoff, and G. Shvets, "Electrical switching of infrared light using graphene integration with plasmonic Fano resonant metasurfaces," *ACS Photonics* **2**(2), 216–227 (2015).
16. H. Schmidt and A. Imamoğlu, "Nonlinear optical devices based on a transparency in semiconductor intersubband transitions," *Opt. Commun.* **131**(4-6), 333–338 (1996).
17. H. Sun, S. Gong, Y. Niu, S. Jin, R. Li, and Z. Xu, "Enhancing Kerr nonlinearity in an asymmetric double quantum well via Fano interference," *Phys. Rev. B* **74**(15), 155314 (2006).
18. R. Asadi, M. Malek-Mohammad, and S. Khorasani, "All optical switch based on Fano resonance in metal nanocomposite photonic crystals," *Opt. Commun.* **284**(8), 2230–2235 (2011).
19. Z. Chai, X. Hu, and Q. Gong, "All-optical switching based on a tunable Fano-like resonance in nonlinear ferroelectric photonic crystals," *J. Opt.* **15**(8), 085001 (2013).
20. Q. M. Ngo, K. Q. Le, T. T. Hoang, D. L. Vu, and V. H. Pham, "Numerical investigation of tunable Fano-based optical bistability in coupled nonlinear gratings," *Opt. Commun.* **338**, 528–533 (2015).
21. Y. Yu, Y. Chen, H. Hu, W. Xue, K. Yvind, and J. Mørk, "Nonreciprocal transmission in a nonlinear photonic-crystal Fano structure with broken symmetry," *Laser Photonics Rev.* **9**(2), 241–247 (2015).
22. C. Wu, A. B. Khanikaev, and G. Shvets, "Broadband slow light metamaterial based on a double-continuum Fano resonance," *Phys. Rev. Lett.* **106**(10), 107403 (2011).
23. J. Gu, R. Singh, X. Liu, X. Zhang, Y. Ma, S. Zhang, S. A. Maier, Z. Tian, A. K. Azad, H.-T. Chen, A. J. Taylor, J. Han, and W. Zhang, "Active control of electromagnetically induced transparency analogue in terahertz metamaterials," *Nat. Commun.* **3**, 1151 (2012).
24. A. E. Miroshnichenko, S. Flach, and Y. S. Kivshar, "Fano resonances in nanoscale structures," *Rev. Mod. Phys.* **82**(3), 2257–2298 (2010).
25. B. Luk'yanchuk, N. I. Zheludev, S. A. Maier, N. J. Halas, P. Nordlander, H. Giessen, and C. T. Chong, "The Fano resonance in plasmonic nanostructures and metamaterials," *Nat. Mater.* **9**(9), 707–715 (2010).
26. C. Genet, M. P. van Exter, and J. P. Woerdman, "Fano-type interpretation of red shifts and red tails in hole array transmission spectra," *Opt. Commun.* **225**(4-6), 331–336 (2003).
27. V. Giannini, Y. Francescato, H. Amrania, C. C. Phillips, and S. A. Maier, "Fano resonances in nanoscale plasmonic systems: a parameter-free modeling approach," *Nano Lett.* **11**(7), 2835–2840 (2011).
28. Y. Francescato, V. Giannini, and S. A. Maier, "Plasmonic systems unveiled by Fano resonances," *ACS Nano* **6**(2), 1830–1838 (2012).
29. Z.-J. Yang, Z.-S. Zhang, L.-H. Zhang, Q.-Q. Li, Z.-H. Hao, and Q.-Q. Wang, "Fano resonances in dipole-quadrupole plasmon coupling nanorod dimers," *Opt. Lett.* **36**(9), 1542–1544 (2011).
30. B. Gallinet and O. J. F. Martin, "Ab initio theory of Fano resonances in plasmonic nanostructures and metamaterials," *Phys. Rev. B* **83**(23), 235427 (2011).
31. A. Lovera, B. Gallinet, P. Nordlander, and O. J. F. Martin, "Mechanisms of Fano resonances in coupled plasmonic systems," *ACS Nano* **7**(5), 4527–4536 (2013).
32. S. Fan, W. Suh, and J. D. Joannopoulos, "Temporal coupled-mode theory for the Fano resonance in optical resonators," *J. Opt. Soc. Am. A* **20**(3), 569–572 (2003).
33. R. E. Hamam, A. Karalis, J. D. Joannopoulos, and M. Soljačić, "Coupled-mode theory for general free-space resonant scattering of waves," *Phys. Rev. A* **75**(5), 053801 (2007).
34. Z. Ruan and S. Fan, "Temporal coupled-mode theory for Fano resonance in light scattering by a single obstacle," *J. Phys. Chem. C* **114**(16), 7324–7329 (2010).
35. L. Huang, Y. Yu, and L. Cao, "General modal properties of optical resonances in subwavelength nonspherical dielectric structures," *Nano Lett.* **13**(8), 3559–3565 (2013).
36. Y. Yu and L. Cao, "Coupled leaky mode theory for light absorption in 2D, 1D, and 0D semiconductor nanostructures," *Opt. Express* **20**(13), 13847–13856 (2012).
37. Y. Yu and L. Cao, "The phase shift of light scattering at sub-wavelength dielectric structures," *Opt. Express* **21**(5), 5957–5967 (2013).
38. Y. L. Yu and L. Y. Cao, "Leaky mode engineering: a general design principle for dielectric optical antenna solar absorbers," *Opt. Commun.* **314**, 79–85 (2014).
39. H. A. Haus, *Waves and Fields in Optoelectronics* (Prentice-Hall, NJ, 1984), Vol. **1**.

## 1. Introduction

Optical Fano resonances bear significant potentials for applications in a wide range of fields including sensing [1–5], lasing [6–8], switching [9–15], nonlinear [16–21], and slow-light device [8, 22, 23]. Physically it arises from the interference of photons that simultaneously interact with two different modes, one with low quality factors (low-Q) and the other high quality factors (high-Q). The interference can facilitate the excitation of the high-Q mode, which could be difficult by the direct incidence of external light, and thereby gives rise to unusual optical responses that are typically manifested by a sharp peak with symmetric or asymmetric profiles embedded in a slow-evolving background spectrum. Controlling the frequency and lineshape of the peak, including symmetry and linewidth, to be whatever pre-specified is very important for the application of optical Fano resonances. However, despite the demonstration of the resonance in numerous systems, such as photonic crystals, plasmonic nanoparticles, metamaterials and so on [24, 25], the capabilities to rationally design optical Fano resonances with arbitrarily pre-specified lineshapes at arbitrarily pre-specified frequencies and frequencies have remained elusive.

One key challenge is the lack of knowledge for the phase associated with optical modes. The phase plays a critical role in the interference involved in optical Fano resonances. Although a variety of approaches have been developed to either simulate or design optical Fano resonances, including optical analog of the Fano model [26–28], coupled oscillator model [29–31], temporal coupled mode theory [32–34], and FDTD simulations, none of them is able to provide unambiguous information for the phases involved. Here we present an approach of deterministic phase engineering that can be used to rationally design optical Fano resonances with arbitrarily pre-specified lineshapes. We demonstrate that the phase difference between a high-Q and a low-Q mode that interfere with each other is solely determined by the difference in the eigenvalue of the two modes. This allows us to deterministically engineer the phase by simply tuning the eigenvalue. We also argue that the frequency of an optical Fano resonance with rationally designed lineshapes can be readily tuned by simply scaling the dimension of the structure involved. We use grating structures as an example to illustrate the notion of deterministic engineering for the rational design of optical Fano resonances with arbitrarily pre-specified symmetry, linewidth, and frequencies.

Our approach of deterministic phase engineering is built upon an intuitive model, coupled leaky mode theory (CLMT), which we have recently developed for the evaluation of light absorption and scattering of dielectric nanostructures [35–38]. The CLMT model considers a dielectric structure, regardless the physical features, as a leaky resonator and its light absorption and scattering as a result of the coupling between incident light and the structure's leaky modes. Leaky modes are natural optical modes with propagating waves outside the structure, and each of them has a complex eigenvalue ( $N_{\text{real}} - N_{\text{imag}}i$ ). The major advantage of the CLMT model is providing capability to evaluate the light-matter interaction contributed by every single mode. This may open up a bottom-up strategy for the rational design of optical structures, in which we can control the optical response of a multiple-mode structure by engineering the contribution from each individual mode.

## 2. Determining the optical phase of leaky modes

We have previously demonstrated that the CLMT model allows us to find out the phase associated with the leaky mode in single nanostructures in spherical or cylindrical shapes [37]. We use one dimensional (1D) dielectric grating structures illuminated by a plane wave in the normal direction [Fig. 1(a)] as an example to illustrate the approach of deterministic phase engineering. For simplicity, we assume the dielectric materials to be lossless with a refractive index  $n = 3.65$  (close to silicon). We also only consider incident light with transverse magnetic (TM) polarization, i.e. the electric field parallel to the longitudinal direction of the grating element. Without losing generality, we assume the element to be

square (thickness versus width  $a/b = 1$ ) and the grating to have a filling factor of 0.83 (width versus period  $b/P = 0.83$ ). We can numerically calculate the eigenvalue and field distribution of leak modes in the grating structure [35]. The quality factor of the mode  $Q$  can be calculated from the real and imaginary parts of the eigenvalue as  $Q = N_{\text{real}}/(2N_{\text{imag}})$ . Figure 1(b) shows the calculated electric field distribution  $E_z$  of typical leaky modes and the corresponding complex eigenvalues are listed in Table 1. Each of the leaky modes is labeled using a mode number  $m$  and an order number  $l$  as  $\text{TM}_{ml}$ , where  $m$  and  $l$  represent the number of maxima in the electric field ( $|E_z|^2$ ) distribution along the  $y$  (horizontal) and  $x$  (vertical) axes, respectively. Depending on the radiative loss, which is indicated by the imaginary part of the eigenvalue, we can divide the leaky modes into two categories,  $\text{TM}_{31}$ ,  $\text{TM}_{32}$ ,  $\text{TM}_{33}$  as high quality factor (high- $Q$ ) modes and  $\text{TM}_{12}$ ,  $\text{TM}_{13}$ ,  $\text{TM}_{14}$  as low quality factor (low- $Q$ ) modes. The high- $Q$  modes have smaller imaginary parts in the eigenvalue and stronger confinement in the eigenfield. We can also divide the leaky modes into even and odd modes based on the symmetry of the eigenfield with respect to the mirror plane parallel to the structure, for instance,  $\text{TM}_{12}$ ,  $\text{TM}_{14}$ ,  $\text{TM}_{32}$  as odd modes and  $\text{TM}_{13}$ ,  $\text{TM}_{31}$ ,  $\text{TM}_{33}$  even modes.

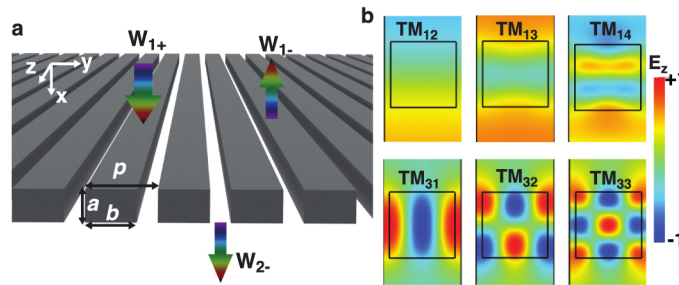


Fig. 1. (a) Schematic representation for the coupling of external electromagnetic waves with one-dimensional grating structures. The coordinate system and the dimension of the grating structure are labeled as shown. (b) Electric field distribution  $E_z$  of typical leaky modes with transverse magnetic (TM) polarization in a square grating. The size ratio  $a/b$  and the filling factor  $b/P$  of the grating are 1 and 0.83, respectively.

**Table 1. Leaky modes of the grating structure**

	Nreal	Nimag	$\theta(\pi)$	Parity
TM12	3.391	0.644	0	odd
TM13	6.625	0.572	0.015	even
TM31	6.755	0.029	0.595	even
TM32	8.205	0.052	0.092	odd
TM14	9.834	0.525	0.025	odd
TM33	10.36	0.062	0.0491	even

The reflection and transmission of the grating can be evaluated using the CLMT model. As shown in Fig. 1(a), we consider the incoming wave for the grating as  $W_{1+}$ , and the outgoing waves as  $W_{1-}$  (reflection) and  $W_{2-}$  (transmission), whose square amplitude represents the power carried. These waves are correlated with each other through coupling with the leaky modes of the grating structure. Intuitively, the incoming wave can couple energy into the leaky mode, and the energy stored in the mode may subsequently radiate out in forms of outgoing waves. For simplicity, let's start with the coupling of one single mode  $\text{TM}_{ml}$ . We may find out the reflection and transmission coefficients of the leaky mode for an incident frequency  $\omega$  (detailed derivative process seen in Appendix A) as

$$r_{ml} = \frac{W_{1-}}{W_{1+}} = e^{i(2\theta_{ml} + \pi)} + \frac{N_{imag}}{i(N_{real} - nka) + N_{imag}} e^{i2\theta_{ml}} \quad (1)$$

$$t_{ml} = \frac{W_{2-}}{W_{1+}} = \pm \frac{N_{imag}}{i(N_{real} - nka) + N_{imag}} e^{i2\theta_{ml}} \quad (2)$$

where  $\theta_{ml}$  is the intrinsic phase of the leaky mode and physically represents the phase change induced by the coupling of electromagnetic waves in or out of the leaky mode.  $N_{real}$  and  $N_{imag}$  are the real and imaginary parts of the eigenvalue of the mode, which can be related with the mode's eigenfrequency  $\omega_{ml}$  and radiative decay rate  $\gamma_{ml}$  as,  $N_{real} = n\omega_{ml}a/c$  and  $N_{imag} = n\gamma_{ml}a/c$ , ( $c$  is the speed of light in vacuum).  $k$  is the wavenumber of the incident light in free space as  $k = \omega/c$ . The  $\pm$  sign in the transmission  $t_{ml}$  is related with the parity of the mode ( $+$  for even mode and  $-$  for odd mode). As indicated by the eigenfields shown in Fig. 1b, the outgoing waves of odd modes at the two sides of the grating have a phase difference of  $\pi$ . We have previously demonstrated that the optical response of a multiple-mode structure is just a simple summation of the contribution from all the individual modes [36, 37]. Equations (1) and (2) can be used to evaluate the reflection and transmission of a Fano resonance that involves two modes (one high- $Q$  mode and one low- $Q$  mode) as

$$r_F = e^{i(2\theta_{ml} + \pi)} + \frac{N_{imag}}{i(N_{real} - nka) + N_{imag}} e^{i2\theta_{ml}} + \frac{N'_{imag}}{i(N'_{real} - nka) + N'_{imag}} e^{i2\theta'} \quad (3)$$

$$t_F = \pm \left[ \frac{N_{imag}}{i(N_{real} - nka) + N_{imag}} e^{i2\theta_{ml}} \pm \frac{N'_{imag}}{i(N'_{real} - nka) + N'_{imag}} e^{i2\theta'} \right] \quad (4)$$

where  $N_{imag}$ ,  $N_{real}$ , and  $\theta_{ml}$  are the eigenvalue and phase of the low- $Q$  mode while  $N'_{imag}$ ,  $N'_{real}$ , and  $\theta'$  belong to the high- $Q$  mode. The term of  $e^{i(2\theta_{ml} + \pi)}$  represents a direct reflection of the incoming wave. Intuitively, the high- $Q$  mode is difficult to be directly excited by incident light and its excitation is likely through an indirect way channeled by a coupling with the low- $Q$  mode. Therefore, there is no direct reflection term contributed by the high- $Q$  mode. The first  $\pm$  sign in the transmission is related with the parity of the low- $Q$  mode and the second is dependent on if the parity of the high- $Q$  mode is the same as that of the low- $Q$  mode ( $+$  for the same and  $-$  for opposite).

We find that the phase difference of the two modes ( $\theta_{ml} - \theta'$ ) can be rigorously determined. Similar to what previously used to the analysis of guided resonances in photonic crystals, we apply the constrain of energy conservation,  $|r_{ml}|^2 + |t_{ml}|^2 = 1$  and  $|r_F|^2 + |t_F|^2 = 1$  to Eqs. (1)-(4). This may give rise to

$$e^{i(2\theta_{ml} + \pi)} = -(r_{ml} \pm t_{ml}) \quad (5)$$

Equation (5) indicates that the optical phase of the high- $Q$  mode is solely determined by the reflection and transmission coefficients of the low- $Q$  mode! This is consistent with the intuitive picture that the excitation of the high- $Q$  mode is mediated by the low- $Q$  mode. We can get more insight by substituting Eqs. (1)-(2) into Eq. (5). We find that the two modes with opposite parities may have identical phase as  $\theta_{ml} = \theta'$  and cannot enable Fano resonances, which is caused by inefficient coupling of the modes due to the opposite parities. For the two modes have the same parity ( $+$  in the parenthesis of Eq. (5)), we may have

$$2\theta' - 2\theta_{ml} = \arctan \frac{2(N_{real} - N'_{real}) / N_{mag}}{[(N_{real} - N'_{real}) / N_{mag}]^2 - 1}, \text{ if } N_{imag}^2 < (N_{real}^2 - N'_{real}^2) \quad (6)$$

$$2\theta' - 2\theta_{ml} = \pi + \arctan \frac{2(N_{real} - N'_{real})/N_{mag}}{[(N_{real} - N'_{real})/N_{mag}]^2 - 1}, \text{ if } N_{imag}^2 > (N_{real}^2 - N'_{real}{}^2) \quad (7)$$

This indicates that the phase difference of the two modes is determined by the difference of the eigenvalue of the two modes. For a structure involving multiple modes, where a high- $Q$  mode may interfere with more than one low- $Q$  modes, to precisely evaluate the phase would require the reflection and transmission contributed from all the related low- $Q$  modes to be taken into account. However, Eqs. (6) and (7) stand as a very good approximation for the scenario where the eigenvalue of the high- $Q$  mode is closer to that of one low- $Q$  modes than the other low- $Q$  modes. The conclusion that the phase difference of the modes is associated with the difference in eigenvalues holds universally regardless the complexity of the structure.

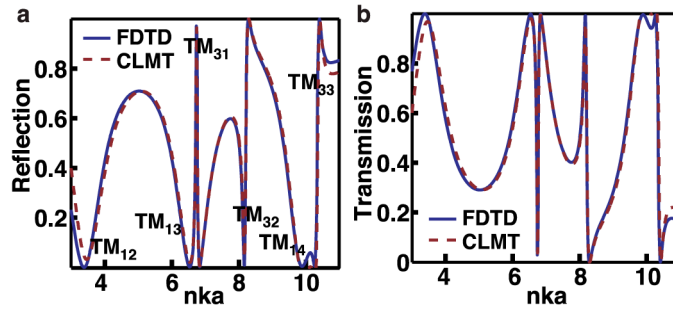


Fig. 2. Comparison of (a) the reflection and (b) transmission spectra calculated by using the CLMT model (dash lines) and FDTD techniques (solid lines).

To confirm the validity of our analysis on the phase difference, we numerically evaluate the spectral transmission and reflection of the grating structure based on Eqs. (3)-(7) and compare the result with what obtained using the well established FDTD techniques. The numerical evaluation involves all the leaky modes listed in Table 1. We first estimate the intrinsic phase of the low- $Q$  modes  $TM_{12}$ ,  $TM_{13}$ , and  $TM_{14}$ . As indicated by the calculated eigenfield given in Fig. 1(b), these modes can be approximately considered as Fabry-Perot resonances in a dielectric slab. And the corresponding intrinsic phase can be correlated to the wave propagation in the vertical direction and is expected to be close to zero (or  $2p\pi$ ,  $p = 1, 2, 3, 4, \dots$ ), similar to what expected in Fabry-Perot resonances. Based on this intuitive picture, we may have  $2\theta_{1l} = (N_{real,1l} - N_{real,12}) + 2\theta_{12}$  for odd modes ( $l = 2, 4, 6, \dots$ ) and  $2\theta_{1l} = (N_{real,1l} - N_{real,12}) + 2\theta_{12} + \pi$  for even modes ( $l = 3, 5, 7, \dots$ ), where  $N_{real,1l} = n\omega_{1l}a/c$  indicates the propagation phase of  $TM_{1l}$  and the term of  $\pi$  is associated with the parity of the mode. As a reasonable approximation, we set the phase of the lowest order mode  $\theta_{12}$  to be zero, and can get the phases of all the low- $Q$  mode as shown in Table 1. We can also find out the phase of the high- $Q$  modes using the strategy given in Eqs. (6) and (7) and the results are given in Table 1 as well. Figure 2 shows the transmission and reflection spectra obtained from the numerical evaluation of Eqs. (3) and (4) using the parameters given in Table 1 (more information of the evaluation seen in Appendix C). Also plotted are the transmission and reflection spectra of the same grating structure calculated by using FDTD techniques. We can find a very nice match between the results obtained from the two different approaches.

### 3. Phase engineering for optical Fano resonances

The correlation of the phase difference to the eigenvalue difference provides useful guidance for the engineering of optical phases to rationally design optical Fano resonances. It essentially converts the engineering of optical phases to the engineering of eigenvalues, the latter of which is much easier. Again we use rectangular grating structures as an example to

illustrate the notion of eigenvalue engineering for the engineering of optical phases. We start with choosing two arbitrary modes with the same parity, for instance,  $TM_{13}$  and  $TM_{31}$  or  $TM_{14}$  and  $TM_{32}$  modes, because the modes with opposite parities cannot enable Fano resonances as discussed in the preceding text. The eigenvalue engineering for the leaky modes in rectangular grating structures can be realized by simply changing the size ratio (thickness versus width) of the rectangular element. We have previously demonstrated that the eigenvalue ( $N_{\text{real}}$ ) of leaky modes in rectangular structures is linearly dependent on the size ratio ( $a/b$ ) and the dependence is associated with the mode and order numbers  $m$  and  $l$  of the mode, approximately as  $N_{\text{real}} \approx (m - 1)\pi a/b + (l - 1)\pi$  [35]. But the imaginary part  $N_{\text{imag}}$  is not very sensitive to the size ratio. Figure 3a shows the  $N_{\text{real}}$  of  $TM_{13}$  and  $TM_{31}$  modes as well as the  $N_{\text{imag}}$  of  $TM_{13}$  mode as a function of the size ratio (without losing generality, the filling factor is arbitrarily set to be 0.83 in this calculation). By substituting the calculated result in Eqs. (6) and (7), we can obtain the phase difference of the two modes as a function of the size ratio as shown in Fig. 3(b). This allows us to engineer the phase difference for control of optical Fano resonances by simply tuning the size ratio. For instance, to engineer the phase difference of the  $TM_{13}$  and  $TM_{31}$  modes to be  $0.5\pi$ ,  $\pi$ , and  $1.5\pi$ , we just need control the size ratio of the rectangular element in the grating structure to be 0.89, 0.98, and 1.08 (the filling factor being 0.83). Figures 3c-3e show the designed optical Fano resonances, which exhibit symmetric or asymmetric lineshapes as expected.

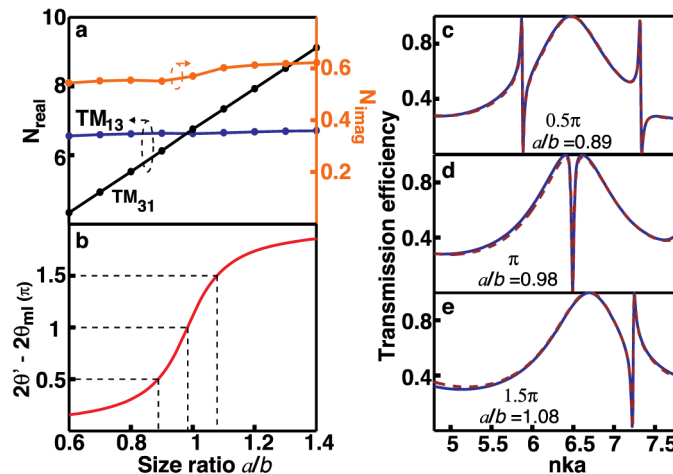


Fig. 3. Phase engineering for the design of Fano resonances with controlled lineshapes. (a) The real part of calculated eigenvalues of  $TM_{13}$  and  $TM_{31}$  as well as the imaginary part of the eigenvalue of  $TM_{13}$  as a function of the size ratio (thickness versus width). Without losing generality, the filling factor (width versus period) of the grating structure involved in the calculation is set to be 0.83. (b) Phase difference between the  $TM_{13}$  and  $TM_{31}$  modes as a function of the size ratio. The dashed lines indicate the size ratio required for phase differences of  $0.5\pi$ ,  $\pi$ , and  $1.5\pi$ , respectively. (c-e) Transmission spectra of the grating structures with the chosen size ratios as indicated in (b). The phase difference and the size ratio used for each grating structure are labeled as shown. The leaky modes are also labeled and the unlabeled peak at  $nka \sim 7.3$  in (c) is contributed by  $TM_{32}$ . The transmission spectra calculated by using the CLMT model (dash lines) and FDTD techniques (solid lines) both are given to further confirm the validity of the CLMT model.

As an additional note, the linewidth and frequency of optical Fano resonances can be independently tuned in a straightforward ways without causing changes in the lineshape. The linewidth is dictated by the radiative loss of the high- $Q$  mode that is related with the imaginary part  $N_{\text{imag}}$  of the modal eigenvalue. And it can be tuned by simply controlling the filling factor (width versus period  $b/P$ ) in grating structures. We find that  $N_{\text{imag}}$  of the leaky modes in grating structures monotonically decrease with the filling factor increasing, while

the real part of the eigenvalue ( $N_{\text{real}}$ ) remains to be pretty much constant regardless of the filling factor as shown in Fig. 4(a). The correlations of  $N_{\text{imag}}$  and  $N_{\text{real}}$  with the filling factor can be understood from an intuitive perspective. The leaky mode may turn to be a guided mode with no radiative loss if the filling factor is equal to 1, and the field confinement is expected to decrease with the inter-element spacing increasing (filling factor decreasing). In contrast, the resonant condition is more related with the dimension of each individual element, instead of the inter-element spacing. The different dependences of  $N_{\text{imag}}$  and  $N_{\text{real}}$  on the filling factor may provide capabilities to tune the linewidth of optical Fano resonances by controlling the period of the grating without causing much change in the phase difference (lineshapes) as shown in Fig. 4(b). Additionally, the frequency of optical Fano resonances can be simply tuned to be arbitrary values by scaling the dimension of the structure involved. All the rational design of optical Fano resonances with arbitrary lineshape and linewidth we have discussed so far use the normalized parameter  $nka$  to be the variable, as shown in Fig. 3 and Fig. 4. For a designed Fano resonance with a fixed value of  $nka$ , its resonant frequency  $\omega$  can be readily tuned to be any arbitrary value by scaling the dimension of the structure.

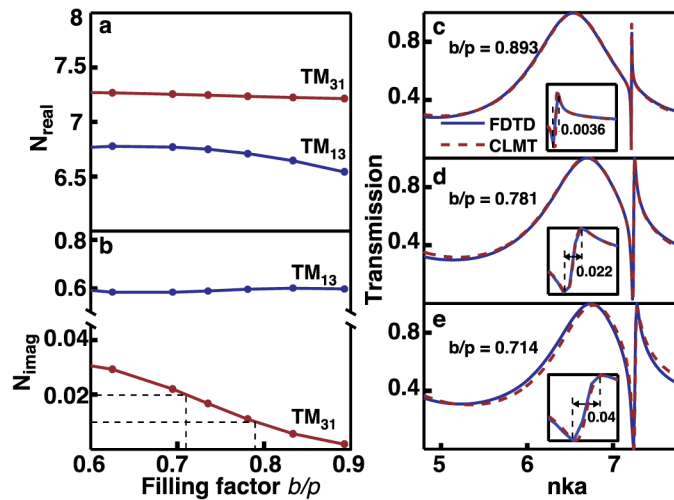


Fig. 4. Control of the linewidth of Fano resonances. (a) The real part and (b) imaginary part of calculated eigenvalues of  $TM_{13}$  and  $TM_{31}$  as a function of the filling factor. The dashed lines indicate the filling factors that should be chosen in order to tune  $N_{\text{imag}}$  to be arbitrarily values 0.02 and 0.011. Without losing generality, the size ratio (thickness versus width versus  $a/b$ ) of the grating element involved in the calculation is set to be 1.08. (c-e) Transmission spectra of the grating structures with the chosen filling factors as indicated in (b). The linewidth of the Fano resonance can be clearly seen in the inset, which is twice as big as  $N_{\text{imag}}$  of the high- $Q$  mode due to the correlation between the quality factor  $Q$  and  $N_{\text{imag}}$  as  $Q = N_{\text{real}}/(2N_{\text{imag}})$ . The size ratio used for each grating structure is labeled as shown.

#### 4. Conclusion

In conclusion, we have demonstrated an approach to deterministically design optical Fano resonances with arbitrarily pre-specified lineshapes, linewidth, and frequencies. The key is to engineer the phase difference of the two modes involved in Fano resonances. We demonstrate that the phase difference between a high- $Q$  mode and a low- $Q$  mode is determined by the eigenvalue difference of the two modes. This is because the high- $Q$  mode is excited indirectly through the coupling with the low- $Q$  mode instead of directly by external incidence. It enables capabilities to deterministically engineer the optical phases by controlling the eigenvalues of optical modes. We use grating structures as an example to illustrate the deterministical design of optical Fano resonances.

## Appendix

### A. Derivative for the reflection and transmission efficiency

The coupling of electromagnetic waves with the leaky mode can be described by formalism similar to conventional temporal coupled mode theory [39]:

$$\frac{da}{dt} = -(i\omega_{ml} + \gamma_{ml})a + \kappa_{ml}W_{1+} \quad (8)$$

$$W_{1-} = C_{W,ml}W_{1+} + C_{1a,ml}a \quad (9)$$

$$W_{2-} = C_{2a,ml}a \quad (10)$$

where  $a$  is the amplitude of electromagnetic fields coupled into the leaky mode from the incident light whose squared magnitude represents the energy stored.  $\omega_{ml}$  and  $\gamma_{ml}$  are the eigenfrequency and radiative decay rate of the leaky mode.  $\kappa_{ml}$  and  $C_{a,ml}$  are the input and output coupling coefficients between the leaky mode and external waves, respectively. We use  $C_{1a,ml}$  and  $C_{2a,ml}$  as the output coupling coefficient for the reflected and transmitted waves because the two waves has a phase difference of  $\pi$  when the leaky mode is an odd mode.  $C_{W,ml}$  is a background reflection coefficient, representing the reflection of the incoming wave without interacting with the leaky mode.

We can find out expressions for the coupling and reflection coefficients based on the principles of energy conservation and time-reversal symmetry. In the case of no incoming wave, from Eqs. (8)-(10), we have

$$a = E_0 \exp(-i\omega_{ml} - \gamma_{ml})t \quad (11)$$

$$W_{1-} = E_0 C_{1a,ml} \exp(-i\omega_{ml} - \gamma_{ml})t \quad (12)$$

$$W_{2-} = E_0 C_{2a,ml} \exp(-i\omega_{ml} - \gamma_{ml})t \quad (13)$$

The leakage rate of the energy must be equal to the power of the outgoing waves

$$\frac{d|a|^2}{dt} = -2\gamma_{ml}|a|^2 = -(|C_{1a,ml}|^2 + |C_{2a,ml}|^2)|a|^2 \quad (14)$$

Based on the symmetry of the eigenfield (see Fig. 1b),  $C_{1a,ml}$  and  $C_{2a,ml}$  are identical when the leaky mode is even but may have a phase difference of  $\pi$  when the mode is odd. Therefore, we may have  $C_{1a,ml} = C_{2a,ml} = \sqrt{\gamma_{ml}}e^{i\theta_{ml}}$  for even leaky modes while  $C_{1a,ml} = \sqrt{\gamma_{ml}}e^{i\theta_{ml}}$  and  $C_{2a,ml} = -\sqrt{\gamma_{ml}}e^{i\theta_{ml}}$  for odd leaky modes.  $\theta_{ml}$  is the intrinsic phase of the leaky mode. Intuitively, it indicates the change in phase when the wave couples in or out the leaky mode.

According to the time-reversal symmetry, when two exponentially growing waves in amplitude of  $W_{1-}^*$  and  $W_{2-}^*$  are input, we would expect the energy stored in the leaky mode exponentially increase as  $a^* = E_0 \exp(i\omega_{ml} + \gamma_{ml})t$  with no outgoing waves. In this case, Eq. (8) can be written as

$$\frac{da^*}{dt} = -(i\omega_{ml} + \gamma_{ml})a^* + \kappa_{1,ml}W_{1-}^* + \kappa_{2,ml}W_{2-}^* \quad (15)$$

$$0 = C_{W,ml}W_{1-}^* + C_{a,ml}a^* \quad (16)$$

We have

$$2\gamma_{ml} = \kappa_{1,ml} C_{1a,ml}^* + \kappa_{2,ml} C_{2a,ml}^* \quad (17)$$

$$C_{W,ml} = -\frac{C_{1a,ml}}{C_{1a,ml}^*} \quad (18)$$

Similar to  $C_{1a,ml}$  and  $C_{2a,ml}$ ,  $\kappa_{1,ml}$  and  $\kappa_{2,ml}$  are identical when the leaky mode is even but may have a phase difference of  $\pi$  when the mode is odd. The only way to satisfy Eq. (17) is  $\kappa_{ml} = C_{a,ml}$ , suggesting that the in-coupling and out-coupling coefficients are identical. From Eq. (18), we have  $C_{W,ml} = e^{i(2\theta_{ml} + \pi)}$ . The phase term of  $2\theta_{ml} + \pi$  can be intuitively understood as resulting from two coupling processes, the incoming wave coupled into the leaky mode and then coupled out to environment as the reflected wave. Each of the coupling causes a phase change of  $\theta_{ml}$  and the extra  $\pi$  phase shift results from the opposite directions of the reflected wave  $W_{1-}$  and the incoming wave  $W_{1+}$ . By considering all of these coefficients, we have

$$a = \frac{\kappa_{ml}}{-i(\omega - \omega_{ml}) + \gamma_{ml}} W_{1+} \quad (19)$$

$$r = \frac{W_{1-}}{W_{1+}} = C_{W,ml} + C_{1a,ml} \frac{a}{W_{1+}} = C_{W,ml} + C_{1a,ml} \frac{\kappa_{ml}}{-i(\omega - \omega_{ml}) + \gamma_{ml}} \quad (20)$$

$$t = \frac{W_{2-}}{W_{1+}} = C_{2a,ml} \frac{\kappa_{ml}}{-i(\omega - \omega_{ml}) + \gamma_{ml}} \quad (21)$$

### B. Derivation for the phase of high-Q modes

Intuitively, we can consider optical Fano resonances as a perturbation caused by high-Q modes for a slow-evolving background spectrum contributed by low-Q modes. We can have the reflection  $r_F$  and transmission  $t_F$  of the Fano resonance as

$$r_F = r_B + r_h \quad (22)$$

$$t_F = t_B + t_h \quad (23)$$

where  $r_B$  and  $t_B$  are the reflection and transmission of the background spectrum,  $r_h$  and  $t_h$  are the reflection and transmission contributed by the high-Q mode. As show in Eq. (3)

$$r_h = \frac{N'_{imag}}{i(N'_{real} - nka) + N'_{imag}} e^{i2\theta'} \quad (24)$$

$$t_h = \pm \frac{N'_{imag}}{i(N'_{real} - nka) + N'_{imag}} e^{i2\theta'} \quad (25)$$

Typically multiple low-Q modes would be involved to contribute the background reflection and transmission, but it is reasonable to consider only the one closest to the high-Q mode when the high-Q modes is substantially further away from other low-Q modes. In this case, we have  $r_F = r_{ml} + r_h$  and  $t_F = t_B + t_h$ . According to the principle of energy conservation,  $|r_{ml}|^2 + |t_{ml}|^2 = 1$  and  $|r_F|^2 + |t_F|^2 = 1$ , we have

$$r_h \cdot r_{ml}^* + r_h^* \cdot r_{ml} + |r_h|^2 + t_h \cdot t_{ml}^* + t_h^* \cdot t_{ml} + |t_h|^2 = 0 \quad (26)$$

As  $t_h = \pm r_h$ . We can rewrite the Eq. (26) as

$$-2|r_h|^2 = r_h \cdot (r_{ml}^* \pm t_{ml}^*) + r_h^* \cdot (r_{ml} \pm t_{ml}) \quad (27)$$

We can also rewrite Eq. (24) as

$$r_h = \frac{N'_{imag}}{i(N'_{real} - nka) + N'_{imag}} e^{i2\theta'} = |r_h| e^{i(\varphi+2\theta')} \quad (28)$$

Where  $|r_h| = \frac{N'_{imag}}{\sqrt{(N'_{real} - nka)^2 + (N'_{imag})^2}} = \cos \varphi$ , and  $\tan \varphi = -\frac{N'_{real} - nka}{N'_{imag}}$

By substituting Eq. (28) into Eq. (27), we have

$$-2|r_h|^2 = |r_h| e^{i(\varphi+2\theta')} \cdot (r_{ml}^* \pm t_{ml}^*) + |r_h| e^{-i(\varphi+2\theta')} \cdot (r_{ml} \pm t_{ml}) \quad (29)$$

By rearrangement we have

$$-2|r_h| = e^{i(\varphi+2\theta')} \cdot (r_{ml}^* \pm t_{ml}^*) + e^{-i(\varphi+2\theta')} \cdot (r_{ml} \pm t_{ml}) \quad (30)$$

which can be rewritten as

$$-2 \cos \varphi = (r_{ml}^* \pm t_{ml}^*) e^{i2\theta'} \cdot e^{i\varphi} + (r_{ml} \pm t_{ml}) e^{-i2\theta'} \cdot e^{-i\varphi} \quad (31)$$

Which can only be satisfied when  $e^{i2\theta'} = -(r_{ml} \pm t_{ml})$

### C. Evaluation of the reflection and transmission spectra of multi-modes structures

We can use the equations for the transmission and reflection of single low-Q and high-Q modes as indicated by Eqs. (1)-(4) to evaluate the optical responses of a structure involving multiple leaky modes. Generally, as what we have demonstrated previously, the optical response of a multiple-mode structure just by simply summing up the contribution of all individual modes involved

$$R = \sum_{m,l} r_{ml} f_{ml} Corr \quad (32)$$

$$T = \sum_{m,l} t_{ml} f_{ml} Corr \quad (33)$$

We include two minor correction factors  $f$  and  $Corr$  for the purpose of obtaining better accuracy in the result. It is worthwhile to point out that the evaluation result without involving the correction factors is also reasonably good but shows some minor inconsistency with the results obtained from FDTD simulations. The term  $f$  is to correct the difference between the incoming wave  $W_{1+}$  and the intensity of the incident light  $I_0$  as  $I_0 = f |W_{1+}|^2$ . Physically, it is associated with the directivity of the coupling between incident light and the leaky mode. We have previously demonstrated that the amplitude  $f$  can be obtained by fitting the absorption spectrum of the structure by introducing a small intrinsic loss (for instance,  $n = 3.65 - 0.01 \cdot i$ ) in the material [35]. The term  $f$  for all the leaky modes of the grating structure is listed in Table 1. We can find there are all very close to be unity.  $Corr$  is a correction term that limits the leaky mode to only couple with incident light close to its eigenfrequency. The involvement of the term  $Corr$  is particularly important for the low-Q modes, whose contribution would be overestimated without involving the term of  $Corr$ .  $Corr$  does not have a rigorous expression, but we have previously found that  $1/[1 + (\alpha - 1)^2]$  for  $\alpha > 1$  or  $1/[1 + (1/\alpha - 1)^2]$  for  $\alpha < 1$  is

a reasonable estimate, where  $\alpha$  indicates the ratio of the incident frequency versus the eigenfrequency as  $\alpha = nka/N_{\text{real}}$ .

### **Acknowledgments**

This work is supported by the start-up fund from North Carolina State University and partially by the National High Technology Research and Development Program (863) of China (No. 2012AA012201). J. L. would like to acknowledge the Chinese Scholarship Council (CSC, No. 201306320036) for financial support.